Image processing- based Lung Tumor-Detection and Classification using 3D Micro-Calcification of CT Images

Revatthy Krishnmurthy
Department of MCA, MEASI Institute of Information Technology, Chennai, India
revatthy11@gmail.com

Abstract - Lung cancer is deadly of all tumor disease with a high death rate as the identification of lung disease at the postponed stage is risky. Hence, the early prediction of lung disease and its treatment is vital to increase the recovery rate. The pattern recognition model based on the micro-calcification of lung CT images aids to classify the lung lesion disease using its texture and statistical features. The features selected are coefficient of reflection and density of mass for the binned lung CT image physical feature measurement that aids in identifying the malignant nodule. Then, the thresholding method is applied with the three-dimensional (3D) sectional Region of Interest (ROI) using the material dimensions. Thus, the lung lump dimension with its physical and statistical features are analyzed using 100 suspected images with ten normal images. This model includes an SVM classifier for the classification of normal and cancer images, exhibiting 98% of accuracy for the proposed system.
Keywords: Lung cancer, CT image, micro-calcification, coefficient, lung bump, lumps, ROI

1. Introduction

. Lung tumor malignancy is not a gender-based disease as it is commonly viewed in both males and females. ICMR- Indian committee of medicinal study is probably the Indian nation that traces over 17 lakhs of tumor cases with malignant death by 2020 [1]. Still, the recovery ratio and its ability to live are enhanced to 18% of patients in detecting the lung lump as urbanized. Lung transmission audition with countrywide statement employs the CT examination and its malignancy rate due to pulmonary disease infection [2].

The pulmonary nodules and micro-calcifications are often categorized based on the two-dimension measure of the dense lung lump, lesion type, infected respiratory region anomaly [3]. The mainframe Computed Tomography (CT) is the top imaging method to detect and diagnose spatial distribution resolution, expense structure, dominant and noninvasiveness of the hollow lung block. CT is a proficient procedure to distinguish the pulmonary protuberance and micro-calcifications of lung nodules [4]. The radiologists utilize the following dataset measures that are unique, specifically location, the size, and surface figure of the nodules utilizing the micro-calcifications to examine the CT diagnosis.

2. Literature Survey:

The thoracic and pulmonary parenchyma feature data with the ribcage airways lung segmentation is followed by the CNN-based Naive Bayes (NB) automated classifier [5]. The classification stage utilizes the NB classifier that significantly contributes to identifying and classifying the reconstructed pulmonary lung air images [6]. The classifier model is pre-trained using the normal and the lung infected patients database to identify and classify the disease stages using the featured datasets. This high-performance feature extraction and classification of Lung tumor or normal images allows the physicians in easy and early prediction of the accurate classification [7]. This results in the ineffective treatment of the pulmonary disease in enhancing the recovery rate of risky lung disease patients with reduced computational cost.

This research work mainly focused on reducing the diagnosis error through rapid computer applications and detecting lung disease with the golden stage classification [8]. The entire chest image, including the pulmonary images, is acquired from the physiologist-friendly and efficient Computed Tomography (CT) device that plays a vital role in early lung disease diagnosis and treatment [9]. As the five pulmonary lobes of the lung regions are closely attached, it is difficult to extract these lobe images separately [10]. In contrast, the entire left lung and right lung images are aided in detecting the lung airways abnormalities and extracting the pulmonary lobes' features using the spatial distribution function. Convolutional Neural Network (CNN) based analysis of the micro-calcifications using the CT medical

ISSN: 0975-3583, 0976-2833 VOL 12, ISSUE 03, 2021

images employing the Deep Learning (DL) tools [11]. The extracting of the feature datasets utilizes the Region of Interest (ROI) with Hounsfield unit absorption/attenuation coefficient of radiation within the tissue micro-calcification is preconditioned and enhanced on training used as a technique for computer-assisted detection.

The CT pulmonary image enhancement and reconstruction produces the grayscale images with the feature characteristics of lung air with high spatial resolution [12]. The lung tissue contrast of morphological structures of the thoracic images helps the specialists in diagnosing and treating all lung diseases more effectively. The extraction of datasets of the thoracic CT images lies in relating the high-quality air volumetric data variation and distribution within the lung respiratory tract involves the feature selection algorithm [13]. Hence, the proposed accurate segmentation of lungs in a pre-processing step includes forward and backward direction correlations for 3D enhanced images. The isotropic pulmonary images are deployed using the multi-layer CNN with max-pooling interconnected nodes within and between layers provide high resolute feature extraction for 3D image reconstruction [14].

3. Methodologies and Existing System:

3.1. Extraction of Lung Ct Images:

The corporal skin texture in the images is used to extract. Initially, the bin of lung lump pixel is performed. The bin crack technique with sub-images, and is helpful to achieve feature extraction, brings away an evaluation on the selected associated image. The pixel binning is highlighted technique and helps in fetching the functional features examine the description of the micro-calcification region area [15]. The reflection coefficients and evaluation of the lung tumor from the CT image utilize the image dispensation process to identify normal or abnormal images.

3.2. Pattern Recognition

Micro-calcification is the lung CT description aids to categorize outweighing the concentration of extra zone in the lung representation. The pattern recognition of the given prototype also helps categorize based on the ROI and represent the appearance of the lung classification. The micro-calcification prototype is relentless for the manifestation coefficients in CT or MRI descriptions to recognize the micro-calcification in 3D picture assists the dominant feature extraction of datasets for the lung tumor classification based on the micro-calcification evaluation.

3.2.1 CT image Feature Extraction:

The malignancy imaging documentation (TCIA) deploys the normal CT lung image. The malignant lung CT image is given in the ordinary and suspected bump difference occurrence, as shown in Figure 1. Its micro-calcification inside ROI marks the intensities that are correlated with the local variance area.

3.2.2. Image Binning:

The CT image representation is absolutely lung image binning with three rows and four columns. The criteria to select the matrix of the CT image binning are as follows.

1. The images to be binned are should have the same size
2. The entire CT picture is considered for the binning with the same rows and columns. Hence, the vast binning parameters at the next stage of binning are organized with mass micro-calcification.
3. Complete CT representation is binned with a small number of rows and columns. Consequently, the binned figure was computed with lung micro-calcification lung lump using three rows and four columns for the analysis.

Figure 1(a): Normal CT of lung Image (b): CT of Malignant Lung Image

The lung micro-calcification represented in 512 × 512 and resized into 512×504 image is depicted in Figure 2(a). The picture is pre-processed to take the external beam cage. The confined lung crater picture is depicted in Figure 2(c). This pre-processing method extracts the thoracic hollow lung space depicted in Figure 2(b). Then the bin picture's primary stage is reduced to the dimension 128 × 168 and is depicted in Figure 3, using figure 2(c), the level-by-level binning.

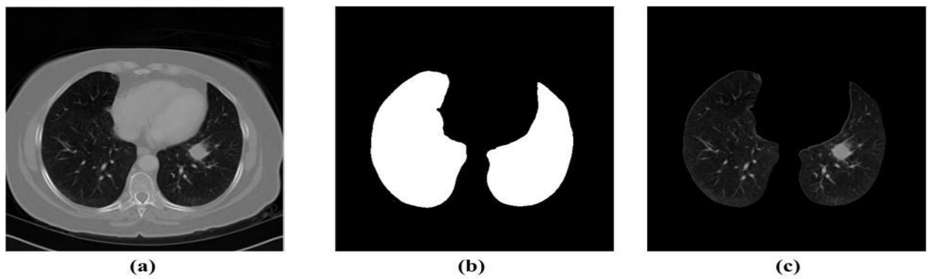

Figure 2: Lung micro-calcification (a) Feature extraction (b) Segmentation of lung opening (c) Lung crater

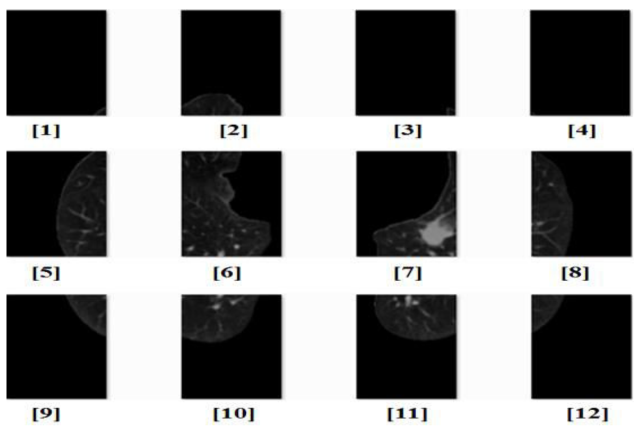

Figure 3: Image of First-level binning of the figure (c) (second-level binning for bin 7)

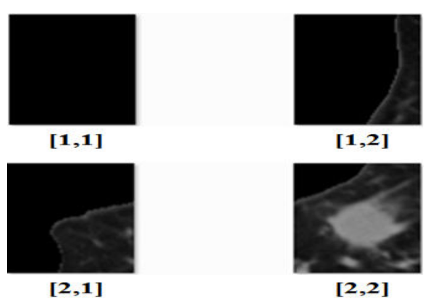

Figure 4: Image of binning the 2nd level [1, 1]; [1, 2]; [2, 1]; [2, 2]

The second level of the storage bin has its dimension of 64 × 84, as depicted in Figure 4.

3.2.3. Reflection Coefficient

The lung tissue pixel-based binning of cancer region enlargement, known as the micro-calcification, is obtained with the thick region due to the calcium depositions. If contaminated lung with such irregularity placed underscan, then body reflects additional power. They reflect power and mirror image coefficient in the graze fraction are elevated using the picture could be model as a two-dimensional purpose. $\mathbf{f}(\mathrm{x,y})$

$$\mathbf{f}(\mathrm{x,y}) = \mathbf{r}(\mathrm{x,y})\mathbf{i}(\mathrm{x,y}) \tag{1.1}$$

Where$\mathbf{i}(\mathrm{x,y})$ is the enlightenment constituent, and $\mathbf{r}(\mathrm{x,y})$is the reflectance module

$0 < \mathbf{i}(\mathrm{x,y}) < \infty, 0 < \mathbf{r}(\mathrm{x,y}) < 1$

r = 0 represent whole assimilation, and **r** = 1 represent whole reflectance.

The coefficient of reflection shows the appropriate curve for the four-sided figure in the small amount technique. The ROI is used to select the region for the manifestation of coefficients for selecting the entrance. The accurate mirror image coefficient assortment is operated as the doorstep in the ROI, selecting the strong-minded utilizing the curvature appropriate of smallest amount four-sided figures columns. It is experiential with a quick difference. The principle coefficients are the most excellent built-in lowering the chi-square approximation. The equation chi-square is described as

$$\sum_i \left(\frac{y - y_i}{\sigma_i}\right)^2 \tag{1.2}$$

Where y is the finest fixed charge, y_i is calculated information, and σ_i is the average departure estimation of y_i

Threshold Segmentation of the ROI segmentation for the image avoids the duplication of the consequent replication using the constant choice is the thresholding. The balancing method segmented pictures to affect the ROI that might be accessible from the whole extracted second-level binning of CT images.

3.2.4. Mass density measurement

The frame of the pixel thickness is basically the micro-calcification evaluates the calcium settlement; the frame thickness is the strong-minded. Micro-calcification raises due to the calcium statement explicitly calcium phosphate and calcium oxalate.

3.2.5. Micro-calcification Pattern Detection and its 3D projection

Micro-calcified ROI assessed image used to provide the 3D projected image from the prediction of ROI to any approach is added to transmit obtainable scientific inspection decoratively added. This 3D forecast aids in regulating the situation and extent of micro-calcified ROI is featured. The 3D forecast of the discarded duplication is shown as the size and elevation of the discarded duplicate, and it establishes a collection of the micro-calcification. A great extent of the micro-calcified ROI region is observed. These statistics and the standards of likeness for the constant figure thickness with the scope of hateful micro-calcification are intended from designing the 3D estimation.

4. Experiment Results and Inferences

Figure 2 (c) is a lung crater image with the spine extracted. The initial near-segmented descriptions of 12 in quantity are shown in Figure 3 with three dins and four posts. The 7th ditched duplicate contains micro-calcified ROI. The box [2, 2] contained the micro-calcification lump. This box is elected for the extra examination. The correct technique of minimum four-sided diminishes with great variations for the replication constants in ROI.

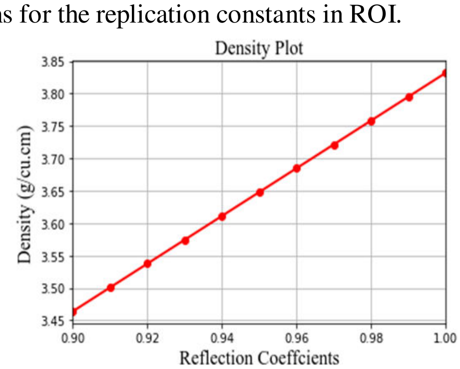

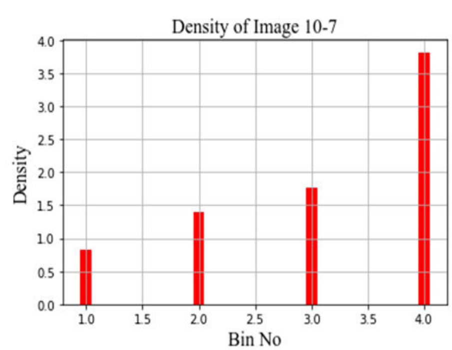

.

Figure 5: Reflection coefficient and density mapping **Figure 6:** Density calculation of second-level bins

4.1. Malignant and benign tumor Classification with SVM: Hundred malignant tumor images and ten normal images are considered for the SVM classifier, the training model with the normal images and tumor images from the database and feature extracted from the database model is stored in the classifier database that is used to compare the testing images. The reflection coefficient and mass density is mapped in figure 5 and density calculation as shown in figure 6

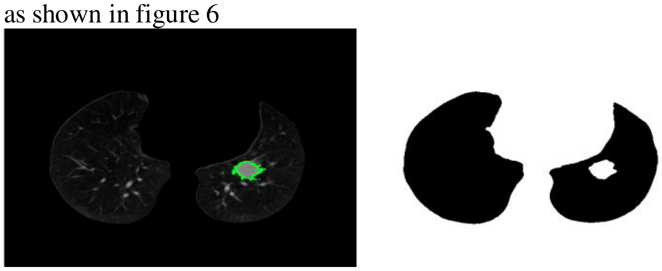

Figure 7: (a) Extract ROI by mapping (b) ROI identification by thresholding

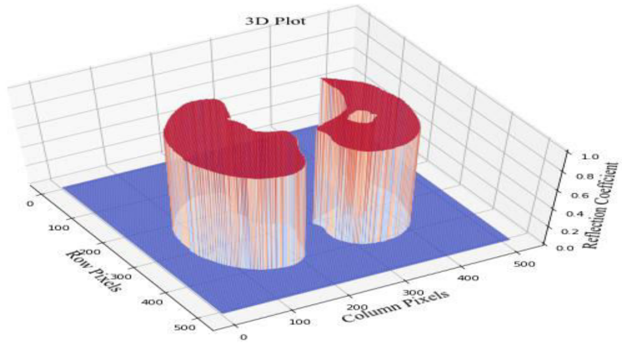

Figure 8: 3-D Detection of lung micro-calcification pattern for bin [2, 2]

4.2. Analysis: The CAD process with bin calculation of the mirror image coefficient, reflection coefficients, and mass densities of micro-calcification is detected and evaluated. The segmentation of the lump productively uses thresholding of mirror image coefficient is performed. Further, the accumulation thickness is the kind of calcium deposit in the lung wall is considered.

The calculation of 3-D representation was not approved in excess concentration with the mirror image coefficient with ROI shown in figure 7. The lump was accurately recognized by extracting the ROI region, and thus 3-d lung tumor is precisely detected in Figure 8.

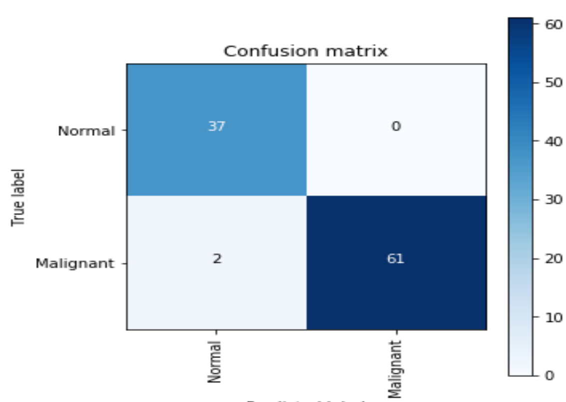

Figure 9: Confusion Matrix of SVM Classifier

ISSN: 0975-3583, 0976-2833 VOL 12, ISSUE 03, 2021

5. Conclusion

CAD process-based bin calculation of the mirror image coefficients of micro-calcification is detected to expect lump extent accurately. From the figure, it is estimated that the concentrations of calcium phosphate at the node prove the lung irregularity is existing. In the benign and malignant tumor detection and classification of lung tumors, the exactness of the classifier reaches 99% accuracy. SVM aids the brilliant precision through 3-D detection methods of feature extraction from CT pictures mirrors image coefficient datasets. This achieves 98% efficiency using the confusion matrix plot, as Figure 9 optimized for diagnosing and categorizing malignant lung tumors.

REFERENCES

1) "Media report (ICMR IN NEWS)," Indian Council of Medical Research Department of Health Research – Ministry of Health & Family Welfare Government of India, (2 February to 8 February 2019)
2) Bach P B, Mirkin J N, Oliver T K, Azzoli C G, Berry D A, Brawley OW, Byers T, Colditz G A, Gould M K, Jett J R et al, "Benefits and harms of CT screening for lung cancer a systematic review", J. Am. Med. Assoc. 3072418–29, 2012
3) Siegel R L, Miller K D, Jemal A, “Cancer statistics”, CA Cancer J. Clin. 68 7–30, 2018
4) Aberle D R, Adams AM, Berg C D, Black W C, Clapp J D, Fagerstrom RM, Green I F, Gatsonis C, Marcus P M, Sicks J D, "Reduced lung-cancer mortality with low-dose computed tomographic screening", New Engl. J. Med. 365 395–409, 2011
5) Ng Q S and Goh V, “Angiogenesis in non-small cell lung cancer imaging with perfusion computed tomography”, J. Thorac Imaging25 142–50, 2010
6) Gibaldi A, Barone D, Gabelli G, Malavasi S and Bevilacqua A, "Effects of guided random sampling of TCCs on blood flow values in CT perfusion studies of lung tumors", Acad. Radiol. 22 58–69, 2015
7) Murugan, S., Anjali, B., & Ganeshbabu, T. R, "Object recognition based on empirical wavelet transform," International Journal of MC Square Scientific Research, Vol. 7(1), pp.77-83. (2015).
8) Rubin GD, “Lung nodule and cancer detection in computed tomography screening”, J Thorac Imaging, 30:130-8, 2015
9) Gruden JF, Ouanounou S, Tigges S, et al, “Incremental benefit of maximum-intensity-projection images on observer detection of small pulmonary nodules revealed by multi-detector CT”, AJR Am J Roentgenol, 179:149-57, 2002
10) National Lung Screening Trial Research T, Aberle DR, Adams AM, et al, “Reduced lung-cancer mortality with low-dose computed tomographic screening”, N Engl J Med, 365:395-409, 2011
11) Moyer VA,“U.S.Preventive Services Task Force. Screening for lung cancer: US Preventive Services Task Force recommendation statement", Ann Intern Med 160:330-8, 2014
12) W. Wang, S. Wu, “A Study on Lung Cancer Detection by Image Processing”, International Conference on Communications, Circuits and Systems, ICCCAS, Proceedings, 2006
13) Veerakumar K., Ravichandran CG "Intensity, Shape and Size Based Detection of Lung Nodules from CT Images", In: Prasath R., Kathirvalavakumar T. (eds) Mining Intelligence and Knowledge Exploration. Lecture Notes in Computer Science, Vol 8284. Springer, Cham, 2013
14) Neelima.S, A. Asuntha “Image Processing used for Lung Cancer Detection in Medical Imaging”, Journal of Chemical and Pharmaceutical Research, 8(4):1044-1049, 2016
15) S. Indira Priyadharsini, N. Mangayarkarasi, L. SaiRamesh, G. Raghuraman, “Lung nodule detection on CT images using image processing techniques”, International Journal of Pure and Applied Mathematics, Vol. 119 No. 7, 479-487, 2018.